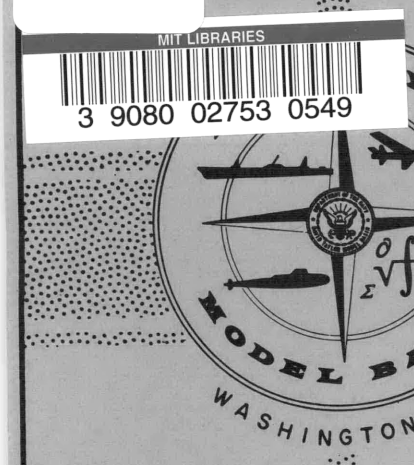

#2

DEPARTMENT OF THE NAVY

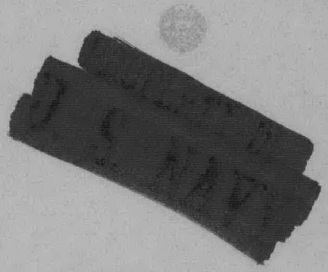

HYDROMECHANICS

O

AERODYNAMICS

O

STRUCTURAL MECHANICS

O

APPLIED MATHEMATICS

O

ACOUSTICS AND VIBRATION

CAVITATION INCEPTION ON THREE-DIMENSIONAL ROUGHNESS ELEMENTS

by

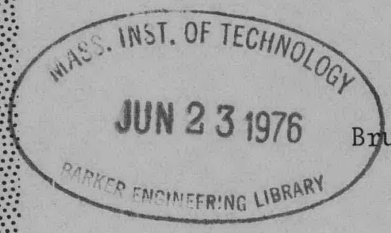

Bruce W. Benson

Distribution of this document is unlimited

HYDROMECHANICS LABORATORY
RESEARCH AND DEVELOPMENT REPORT

May 1966

Report 2104

DAVID TAYLOR MODEL BASIN
WASHINGTON, D. C. 20007

CAVITATION INCEPTION ON THREE-DIMENSIONAL ROUGHNESS ELEMENTS

by

Bruce W. Benson

May 1966

Report 2104
S-F013 02 04
Task 1712

TABLE OF CONTENTS

LIST OF FIGURES

LIST OF TABLES

ABSTRACT

Cavitation inception velocities have been measured for the flow over three-dimensional roughness elements, embedded in a boundary layer on a flat plate, in the 36-inch water tunnel at the David Taylor Model Basin. The roughness elements considered are right circular cylinders, cones, and hemispheres whose heights vary from one-thirty-second to three-forths of an inch. Cavitation inception number, based on tunnel velocity, is plotted as a function of the ratio of roughness height to boundary layer thickness. This resulted in separate curves for each test velocity. When, however, the cavitation number was computed on the basis of the velocity within the boundary layer at the tip of the roughness, the cavitation number was found to be primarily a function of the local Reynolds number, based on roughness height and local velocity. Of the three roughness geometries, the cylinders produced the largest cavitation numbers; the hemispheres, the smallest.

ADMINISTRATIVE INFORMATION

This project was sponsored by the Bureau of Ships under Subproject S-F013 02 04, Task 1712.

INTRODUCTION

The development of high-speed ships and hydrofoils and the increase in size of sonar domes, control surfaces, and propulsion devices have emphasized the problem of cavitation and associated deteriorating effects. Cavitation precipitates such problems as loss of efficiency, noise, vibration and fatigue, reduction of or loss of control, and material damage. The inception of cavitation is a phenomenon governed by both the physics of the flow and the physics of the fluid and has been studied extensively from many approaches. Although much has been determined by these efforts, attempts to develop laws for scaling cavitation data from model to full scale and from environment to environment have not been successful. The characteristics of the array of physical properties affecting cavitation inception is statistical at best and, consequently, so is the prediction of cavitation inception.

A problem of growing concern to the Navy and one that has been little investigated is that of cavitation on small roughnesses on the surface

of flow bodies such as sonar domes and hydrofoils. The inception of cavitation on rough bodies occurs at speeds much below the critical speed intended in the original design of the body.

J.W. Holl,[1] of the Ordnance Research Laboratory of the Pennsylvania State University, performed an experiment in which he observed the effect on cavitation inception of two-dimensional roughness elements submerged in the boundary layer of a flat plate. In addition, he developed a relationship with which the flat plate data could be applied to a general flow-surface of known pressure, velocity, and boundary layer characteristics. It was the purpose of the present investigation to expand Holl's data by similarly investigating cavitation on three-dimensional roughness elements of various shapes, sizes, and patterns. The ultimate objective was to develop methods for predicting the effects of various types of roughness on cavitation inception of full-scale flow surfaces and for providing surface finish criteria for hydrodynamic bodies.

BOUNDARY LAYER AND CAVITATION PARAMETERS

It was the primary purpose of this work to develop the relation between the incipient cavitation number σ_{iR} of a roughness and the relative height of the roughness to the boundary layer thickness h/δ at the location of the roughness.

With reference to Figure 1, a relationship of the form

$$\sigma_{iR} = f\,[h/\delta,\ U] \qquad [1]$$

where U is the free-stream velocity above the test area, can be developed from measured cavitation inception characteristics of a variety of shapes and sizes of roughnesses situated in the boundary layer of a flat plate. The incipient cavitation number σ_{iR} of a roughness is commonly defined as

$$\sigma_{iR} = \frac{p_i - p_v}{\frac{\rho}{2} U_i^2} \qquad [2]$$

---

[1]References are listed on page 30.

where p_i and U_i are the free-stream static pressure and velocity at a height δ above the test area and are measured at the instant of cavitation inception on the roughness;

p_v is the local vapor pressure of the water; and

ρ is the water density.

A close approximation of the velocity distribution in a fully developed turbulent boundary layer on a flat plate is given by

$$\frac{u}{U} = \left(\frac{y}{\delta}\right)^{1/m} \qquad [3]$$

where u is the mean velocity component at height y above the surface and
m is the power which satisfies the particular measured velocity profile.

The functional relationship of Equation [1] can now be developed from pressure and velocity measurements by evaluating Equations [2] and [3] for σ_{iR} and h/δ, respectively.

Cavitation inception occurs in the minimum pressure area of a "smooth" body moving through liquid when that pressure is dynamically reduced to some critical pressure, for example the local vapor pressure. This flow can be described by the incipient cavitation number of the smooth body σ_{iSB}

$$\sigma_{iSB} = \frac{p_{i\infty} - p_v}{\frac{\rho}{2} U_{i\infty}^2} \qquad [4]$$

where $p_{i\infty}$ is the static pressure of the undisturbed free stream at the depth of the body and at the instant of cavitation inception, and

$U_{i\infty}$ is the speed of the body at the instant of cavitation inception.

However, the presence of roughness in the boundary layer of a submerged body, such as is shown in Figure 2, causes further dynamic reductions in local static pressures. Depending on the roughness characteristics and their location on the body, local cavitation can occur at speeds well below those required to achieve smooth body cavitation. The incipient cavitation number of a rough body σ_{iRB} has been developed by Holl[1] in terms of the smooth body pressure coefficient C_{pSB} and the incipient cavitation number

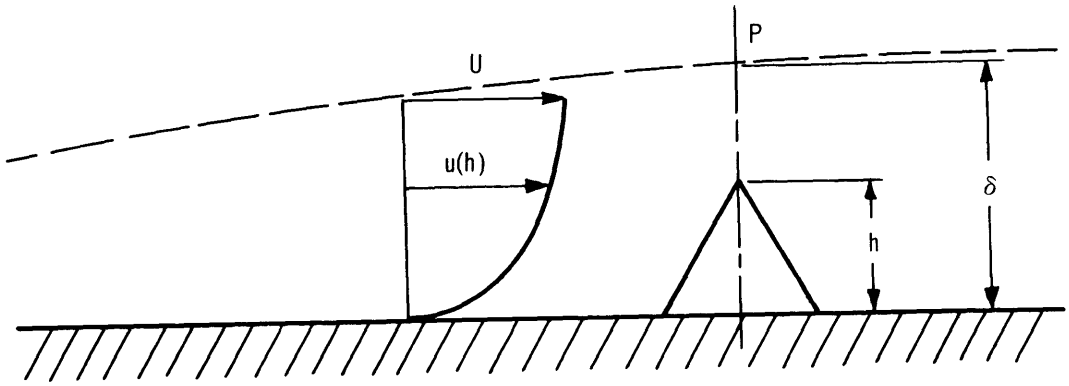

Figure 1 - Roughness in Boundary Layer of Flat Plate

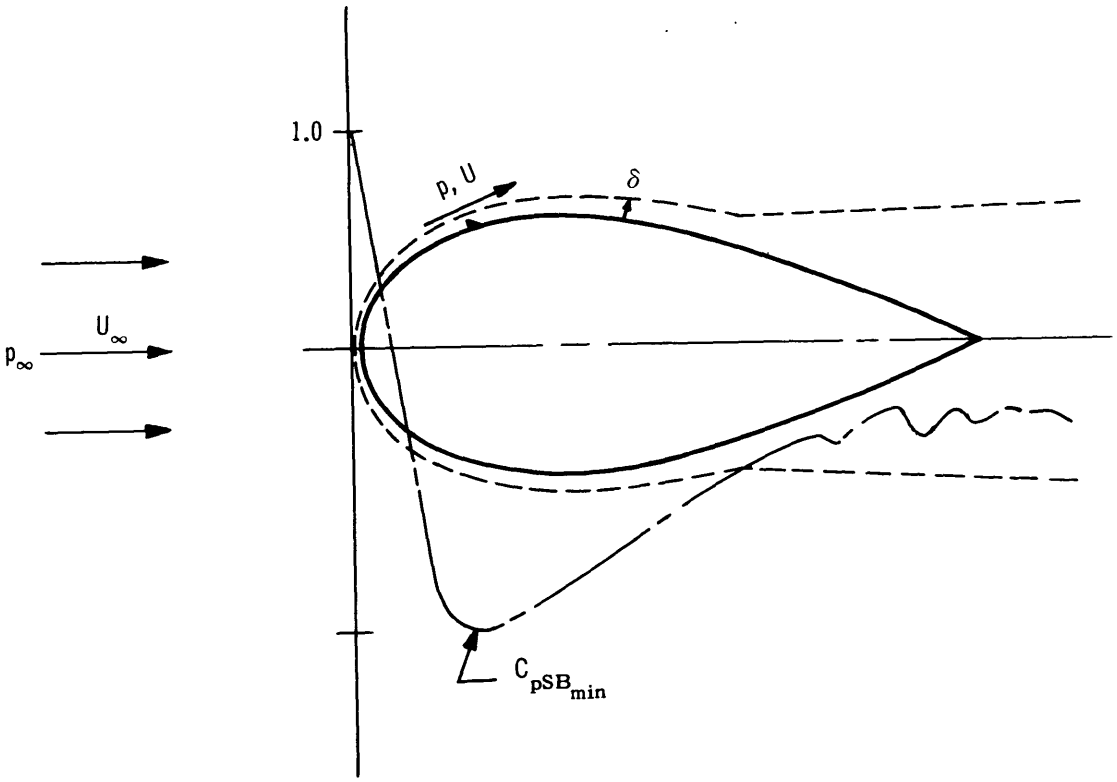

Figure 2 - Typical Flow Body with Roughness

of the roughness σ_{iR} as determined from the flat plate experiment.

$$\sigma_{iRB} = - C_{pSB} + [1 - C_{pSB}] \sigma_{iR} \quad [5]$$

and

$$C_{pSB} = \frac{p - p_\infty}{\frac{\rho}{2} U_\infty^2} \quad [6]$$

where p_∞ is the static pressure of the undisturbed free stream at the depth of the body,

U_∞ is the speed of the body, and

p is the static pressure on the surface of the smooth body at the location of concern.

The cavitation inception speed of general flow bodies whose roughness, pressure, and boundary layer characteristics are known can be determined from Equation [5]. However, since the scaling of cavitation results, from laboratory to full scale, involves variables not implicit in the preceeding definitions, the predicted cavitation speeds are only approximate.

EXPERIMENT

The experiment was conducted in the 36-inch water tunnel at the David Taylor Model Basin and consisted of observing the point of cavitation inception (and disappearance) on various shapes, sizes, and patterns of three-dimensional roughness elements submerged in the boundary layer of a flat plate.

APPARATUS

The variable pressure and velocity water tunnel is a vertical closed-circuit system.[2] The primary loop of the tunnel is about 68 ft long and 28 ft 6 in. above the ground and the inside diameter of the test section is approximately 36 in. Maximum water speed through the test section is 80 ft/sec and the static pressure at the test section centerline can be varied from 2 psia to 60 psia. In addition, a vertical resorber extends 70 ft below the ground level. The function of the resorber is to dissolve a large portion of gas, freed in other parts of the tunnel, by subjecting

it to high pressure for a period of time. As the aerated water passes through the resorber the smaller bubbles in the spectrum are eliminated.

The flat plate boundary layer was developed on a 10-ft-long stainless steel plate. As shown in Figure 3, the plate was supported, on side rails, in the horizontal bisector plane of the tunnel. Figure 4 is a front view photograph of the plate installation. The static pressure at the test station and the longitudinal pressure gradient were monitored by two, parallel rows of pressure taps in the upper surface of the plate; see Figure 3. These taps were situated along the sides of a removable surface in the plate. The tubing from the pressure taps was brought aft in machined grooves in the underside of the plate. These grooves were filled with epoxy and finished flush with the plate surface. The surface plate contained a pattern of screw holes in which the roughness elements were attached; see Figure 5. The leading edge of the plate was a NACA 16-018 foil shape and the trailing edge was approximately a 1-ft taper to a 1/32-in. radius at the tip. A pitot (Prandtl) tube was suspended from the top of the tunnel to measure the free-stream velocity above the plate. A total-pressure traversing probe was projected up through the plate's surface, in the vicinity of the test section, to measure the velocity profile of the boundary layer. A hollow foil, projecting from the bottom of the plate to a sealed access in the bottom of the tunnel, served as a housing for static pressure tubing and for the control stem of the boundary layer probe.

Table 1 shows the shapes and sizes of the stainless steel roughness elements tested for cavitation inception characteristics. Figure 6 is a photograph of the three shapes.

INSTRUMENTATION

Since all measurements were made under steady or near-steady conditions, mercury manometers were used to sense the pressure signals from the pitot tube, boundary layer probe, and static taps in the plate. In addition, the velocity of the approaching fluid could be determined from the pressure drop across the converging section of the tunnel, upstream of the plate leading edge. These pressures were picked up by piezometer rings which encircled the tunnel at two cross sections of the convergence

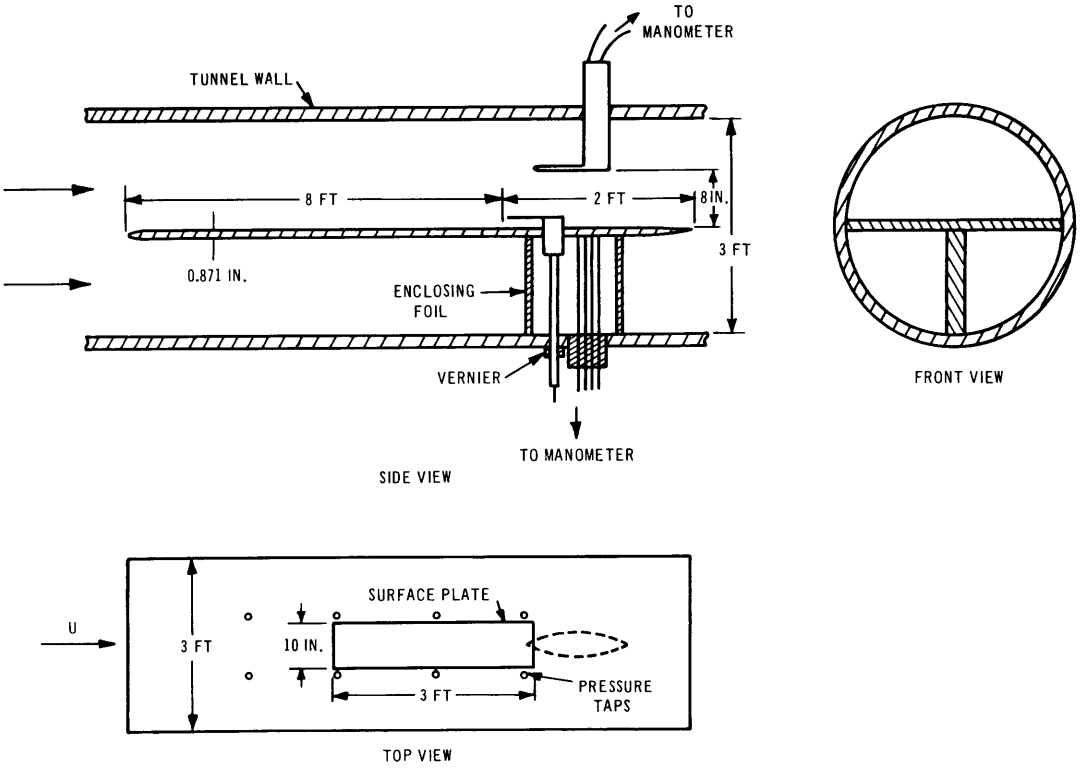

Figure 3 - Schematic of Apparatus

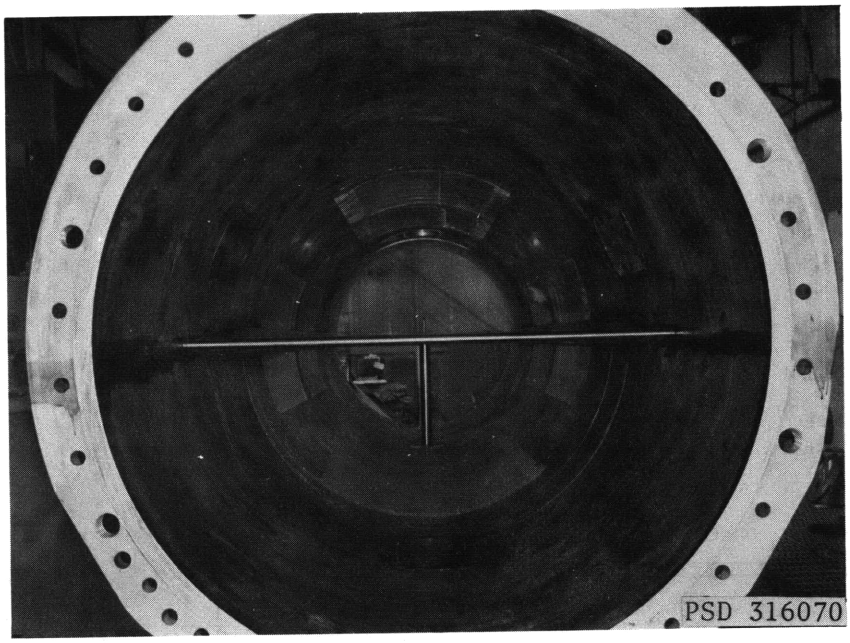

Figure 4 - Front View of Plate in Water Tunnel

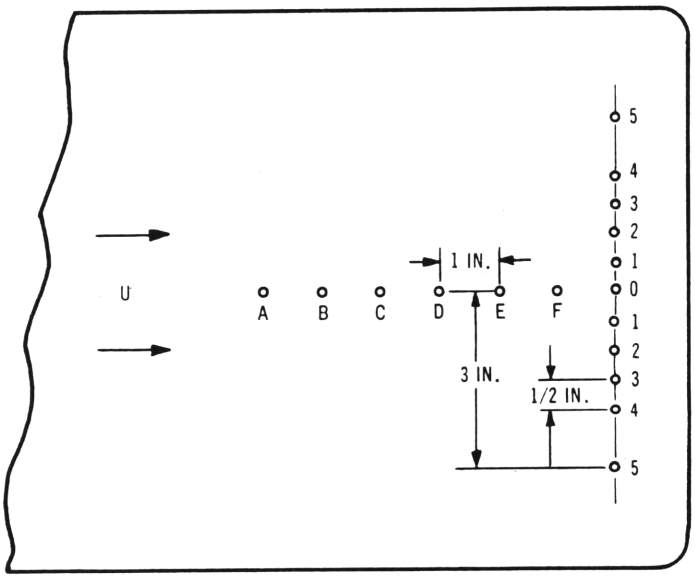

TRANSVERSE PATTERN		LONGITUDINAL PATTERN	
SETTING	POSITION	SETTING	POSITION
1	5-0-5	1	A-D-O
2	4-0-4	2	C-E-O
3	3-0-3	3	E-F-O
4	2-0-2		
5	1-0-1		

Figure 5 - Roughness Patterns in Surface Plate

TABLE 1

Sizes of Roughnesses

Size / Shape	h_1	h_2	h_3	h_4	h_5	h_6
D=h	3/4	1/2	3/8	1/8	1/16	1/32
D=h	3/4	1/2	1/4	1/8	1/16	1/32
D=2h	3/4	1/2	1/4	1/8	1/16	1/32

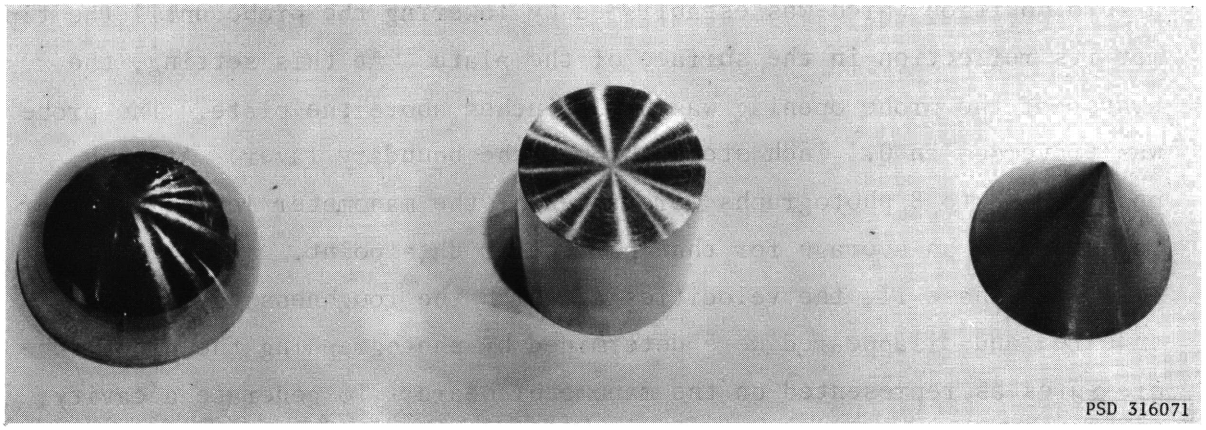

Figure 6 - Three Roughness Geometries Tested for Cavitation Inception Characteristics

and were transmitted to the manometer. A mercury barometer provided the atmospheric pressure, corrected for temperature. The calibrated pitot tube was used as the standard for correcting all other measurements. Pressure measurements were obtained from photographs of the manometer board.

PROCEDURE

The experiment was divided into two phases. In phase I, the mean velocity profile across the boundary layer of the plate was measured for a sequence of free-stream velocities from 20 ft/sec to 60 ft/sec in increments of 5 ft/sec. During this phase, there were no roughnesses on the plate. In phase II, observations were made of cavitation inception velocities of both single roughness elements and patterns of roughnesses situated on the plate. The roughnesses were located approximately eight feet downstream of the leading edge and symmetrical about the center line of the plate; see Figures 3 and 5. The purpose of measuring the velocity profile was (a) to determine the boundary layer thickness, δ, and (b) to determine the magnitude of the mean velocity component at the level of the roughness height, h. Instantaneous readings of all active manometer tubes were recorded on film.

In phase I, the boundary layer probe was traversed vertically from a zero position which was established by lowering the probe until the tip met its reflection in the surface of the plate. At this setting, the center of the probe opening was 0.033 inches above the plate. The probe was traversed in 0.1 inch steps through the boundary layer. At each position, 5 to 8 photographs were taken of the manometer levels in order to determine an average for that particular data point.

In phase II, the velocities at which the roughness cavitation appeared and disappeared were determined by photographing the pitot tube pressures as represented on the manometer board. To generate a cavity, the desired tunnel velocity was established and the tunnel static pressure was lowered until a cavity appeared on the roughness element being tested. This flow condition was held fixed for several minutes to allow the tunnel nuclei to stabilize or adjust to the "new" ambient pressure. The tunnel pressure, only slightly below the inception point, was then very slowly

raised until the cavity disappeared. At this instant, the manometer levels were photographed. This procedure was repeated 5 to 8 times for each particular roughness element and velocity setting. In this experiment, the cavities would appear by bursting into a finite size and would disappear or collapse from a finite size. Their appearance and disappearance was further identified by a high frequency buzzing which was audible outside the test section.

During phase II, the air content of the tunnel water was lowered and maintained between 12 and 18 percent of saturation at the running temperature. This was done to minimize the number of large bubbles which tended to explode in transit through the low pressure of the test section and obscure visibility.

The tunnel was opened several times each day to change or adjust the roughnesses being tested and the air content was determined with the Van Slyke Meter subsequent to each closing. At the end of each test day, the tunnel water was deaerated for several hours to dispell the air absorbed during the testing. It was found that the air content increased only 4 to 6 percent in a day's time.

LIMITATIONS

Some of the difficulties encountered during the experiment were as follows:

(a) The minimum static pressure at the test section was limited to about 3.7 psia. At pressures below this value, tiny air bubbles in the top of the manometer and pitot tubing would suddenly expand and alter the water head on the mercury columns.

(b) The view of the camera, which was used to photograph the manometer levels, was limited to a pressure differential reading equivalent to about 60 ft/sec in free-stream velocity.

(c) The unsteadiness in the tunnel velocity and pressure increased with the mean velocity. All readings were made under "steady-state" conditions. At the lower velocities, small, slow variations in the above properties were accurately monitored by the manometer levels. As the velocity was increased into the 50 ft/sec to 60 ft/sec range, the fluctuations increased in magnitude and were characterized by occasional jumps

in the mercury levels. However, this slightly erratic motion was not considered critical for average readings were acquired by taking a series of photographs of each intended data point.

RESULTS

The boundary layer measurements discussed in the previous section are plotted in Figures 7 through 10. In Figure 7, the ratio, u/U, is plotted on log-log paper as a function of distance, y, above the plate. The point of interception of a straight line through the data points with the horizontal line, u/U = 1, was considered to be the boundary layer thickness δ, corresponding to the particular ambient velocity. As shown in Figure 8, the boundary layer thickness varies from 1.12 inches at a velocity at 20 ft/sec to 1.22 inches at a velocity of 60 ft/sec. The power, m, of Equation [3] was determined by measuring the slopes of the straight lines of Figure 7. This equation is compared with the data points in Figure 9. In Figure 10, u is plotted against y on rectangular coordinates to illustrate the magnitude of u for the various free stream velocities.

The cavitation data of phase II are presented in Figures 11 through 15. Figures 11 through 13 show the relationship between the incipient cavitation number, σ_{iR}, of the three shapes of single roughnesses and their relative heights, h/δ. It can be seen that the inception number increases with size, velocity, and with "sharpness" of the roughness element.

In phase II, both transverse and longitudinal lines of roughnesses were tested for cavitation characteristics. Figure 5 shows the array of patterns used and Figures 14 and 15 illustrate the effects of the proximity of the elements on the cavitation inception number. In the transverse pattern, σ_{iR} increases with a decrease in element separation. In the longitudinal pattern σ_{iR} decreases with a decrease in element separation.

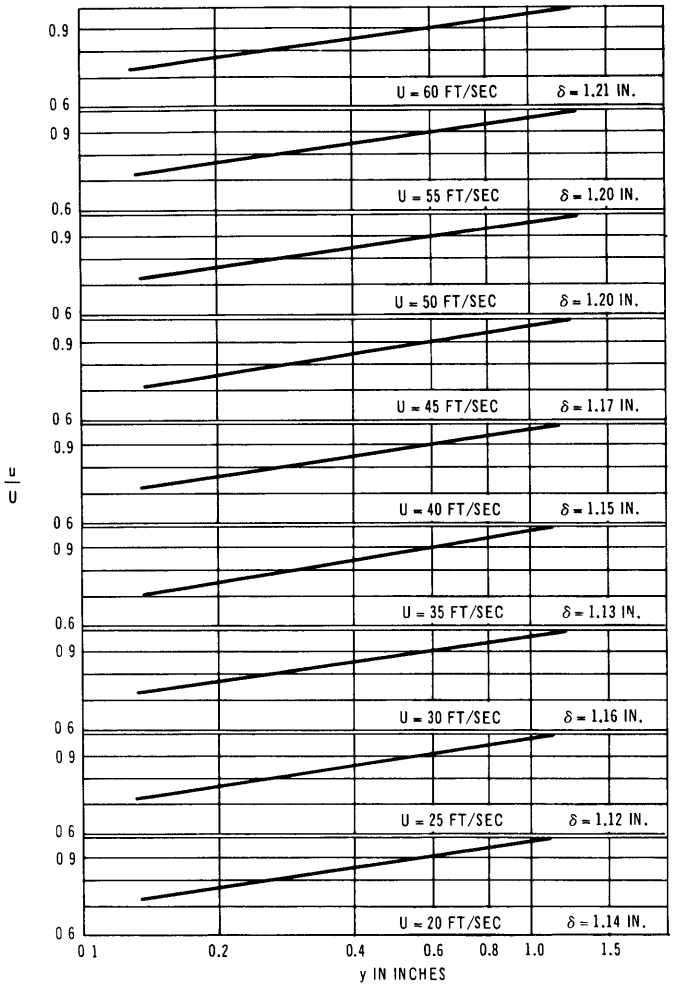

Figure 7 - Boundary Layer Velocity Profile Above Surface of Flat Plate

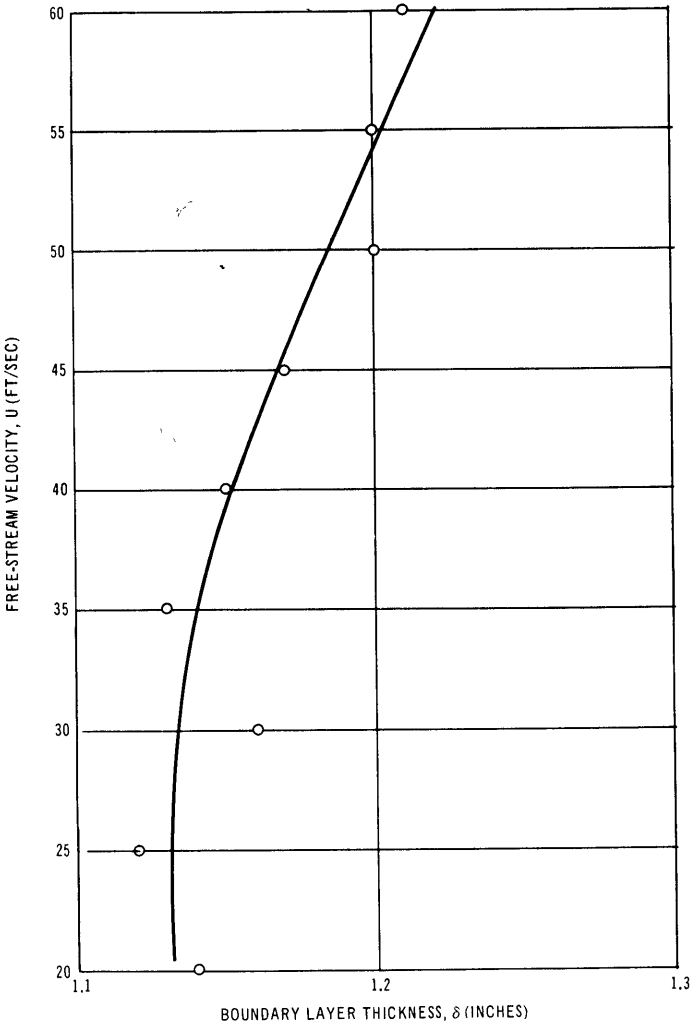

Figure 8 - Flat Plate Boundary Layer Thickness as a Function of Velocity

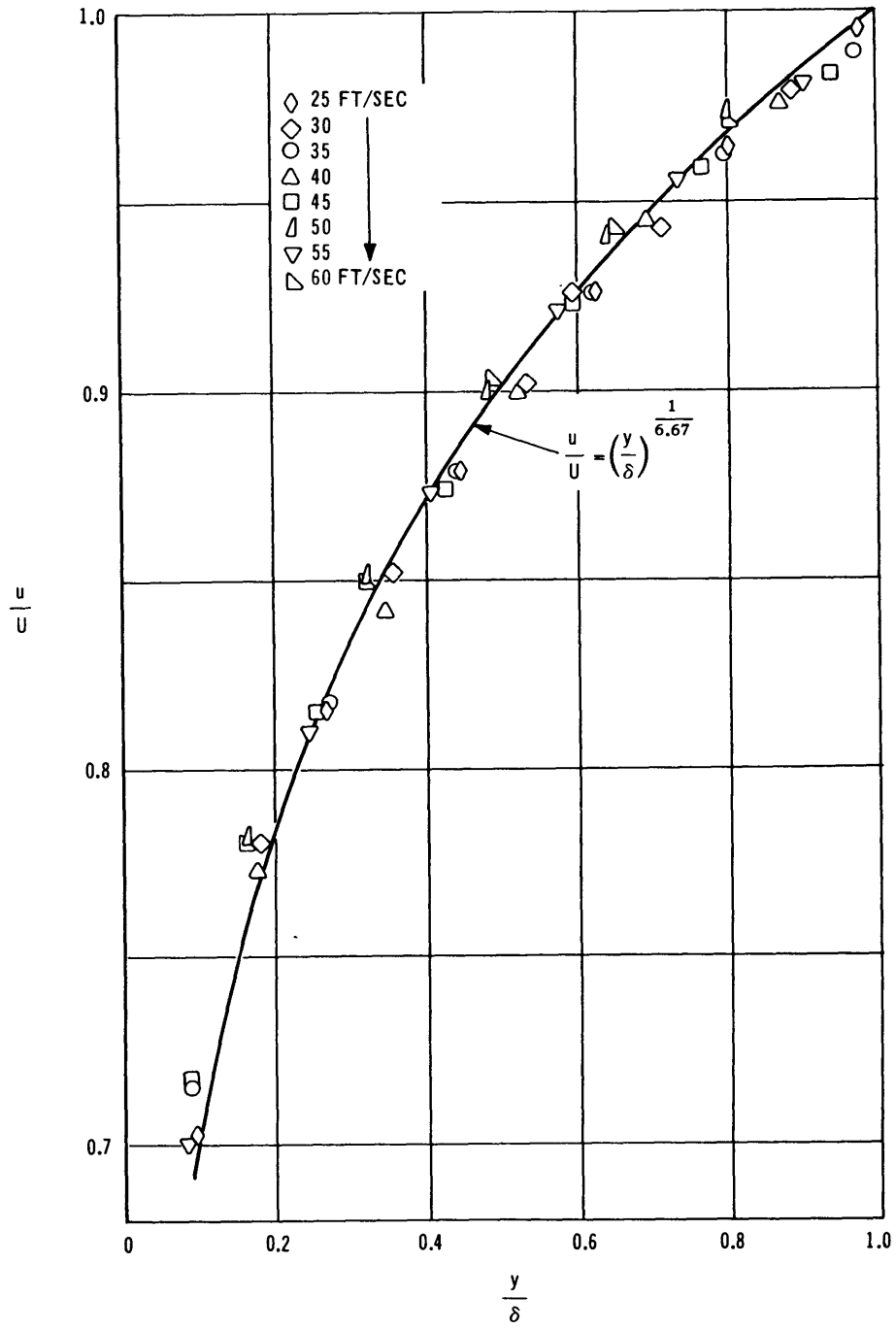

Figure 9 - Comparison of Data with Power Law Representation of Boundary Layer Velocity

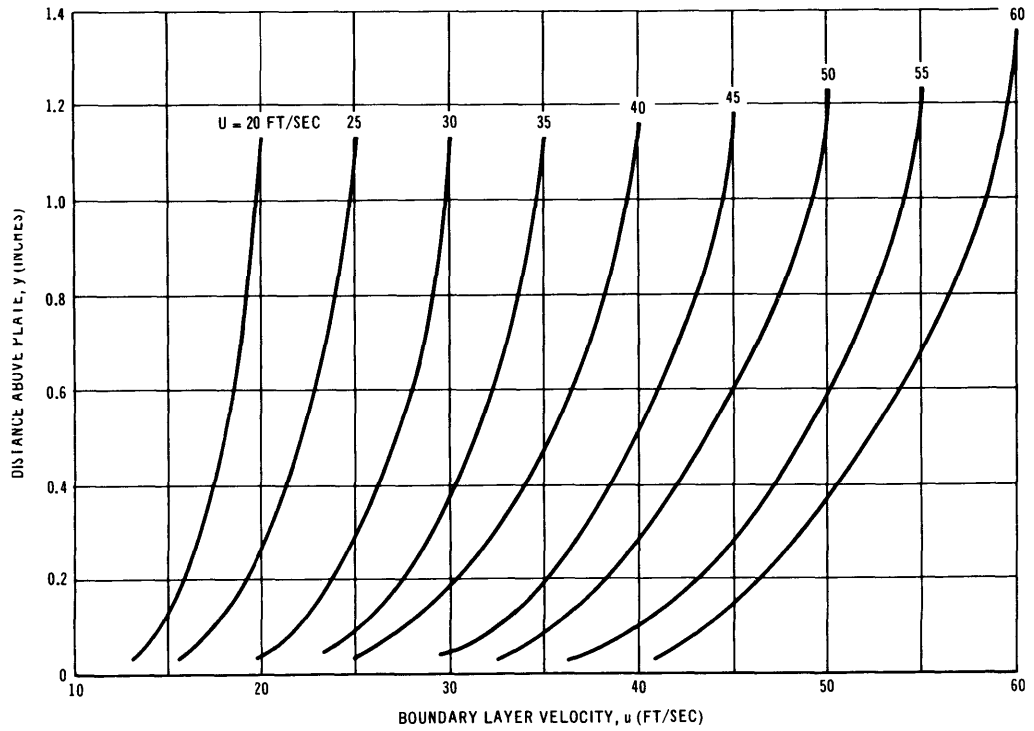

Figure 10 - Comparison of Boundary Layer Velocity Profiles

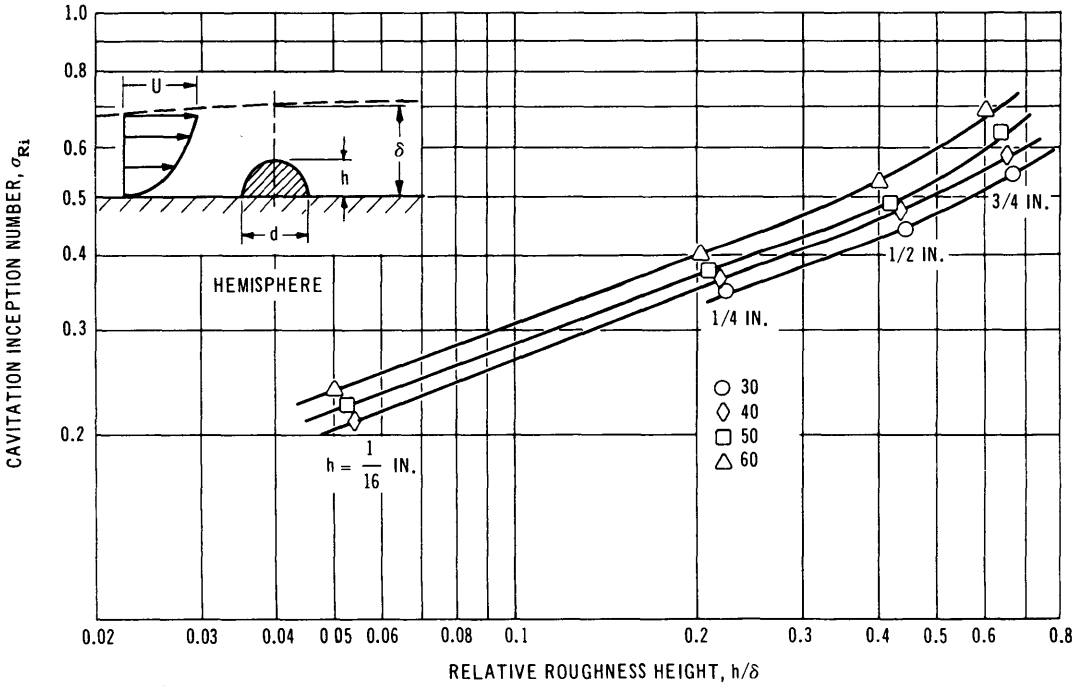

Figure 11 - Cavitation Inception Number as a Function of Relative Roughness Height of a Hemisphere

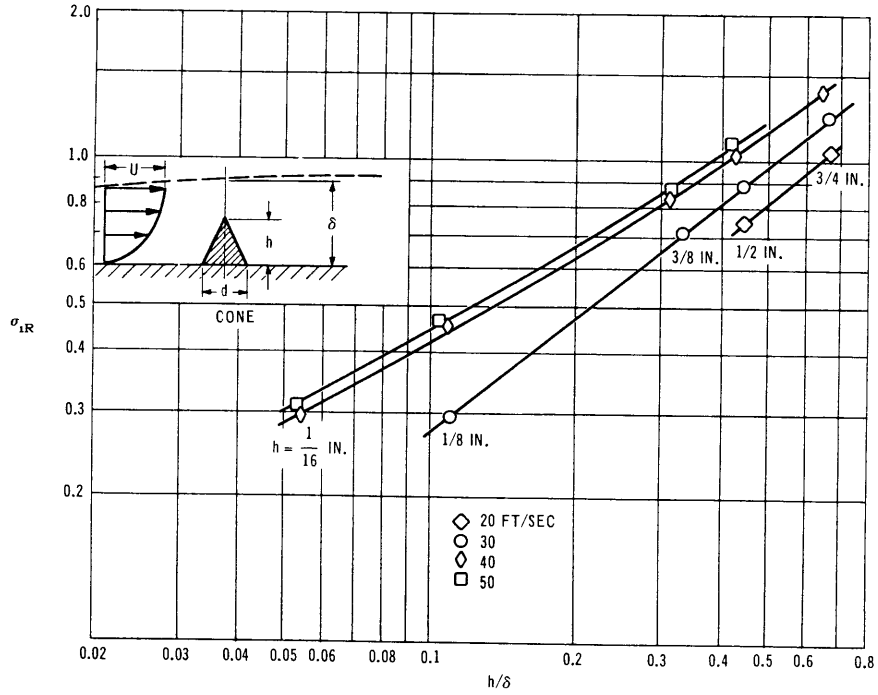

Figure 12 - Cavitation Inception Number as a Function of Relative Roughness Height of a Cone

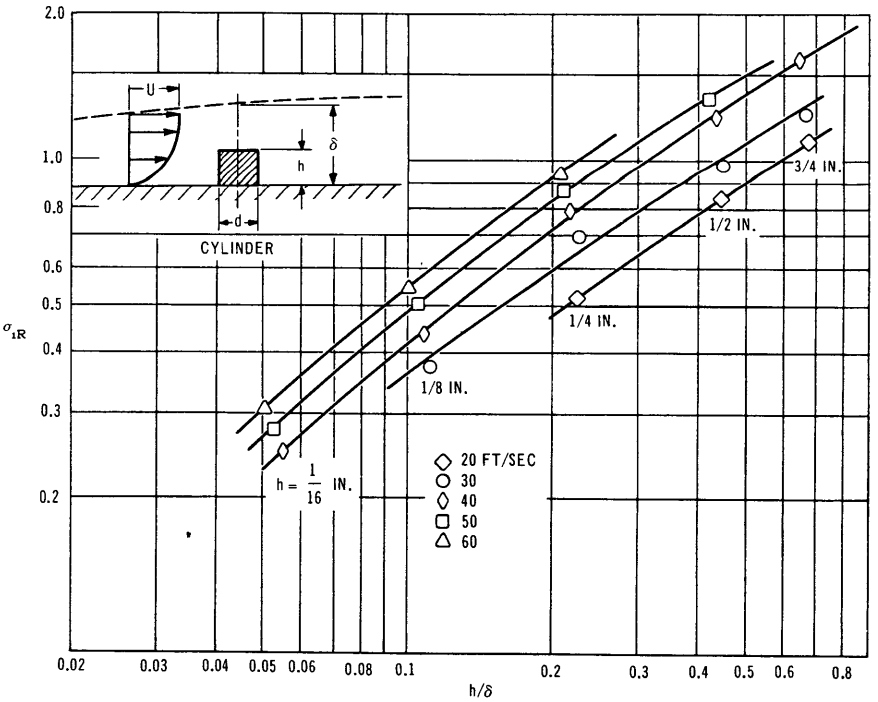

Figure 13 - Cavitation Inception Number as a Function of Relative Roughness Height of a Cylinder

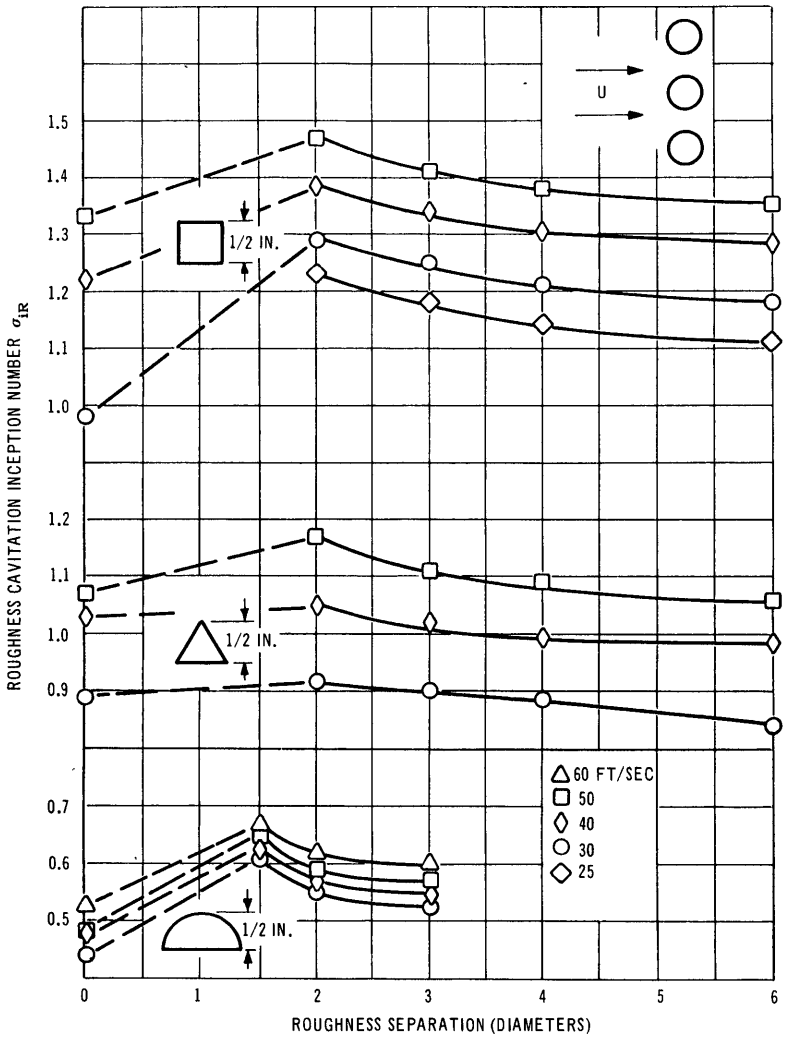

Figure 14 - Cavitation Inception Number as a Function of Transverse Roughness Separation

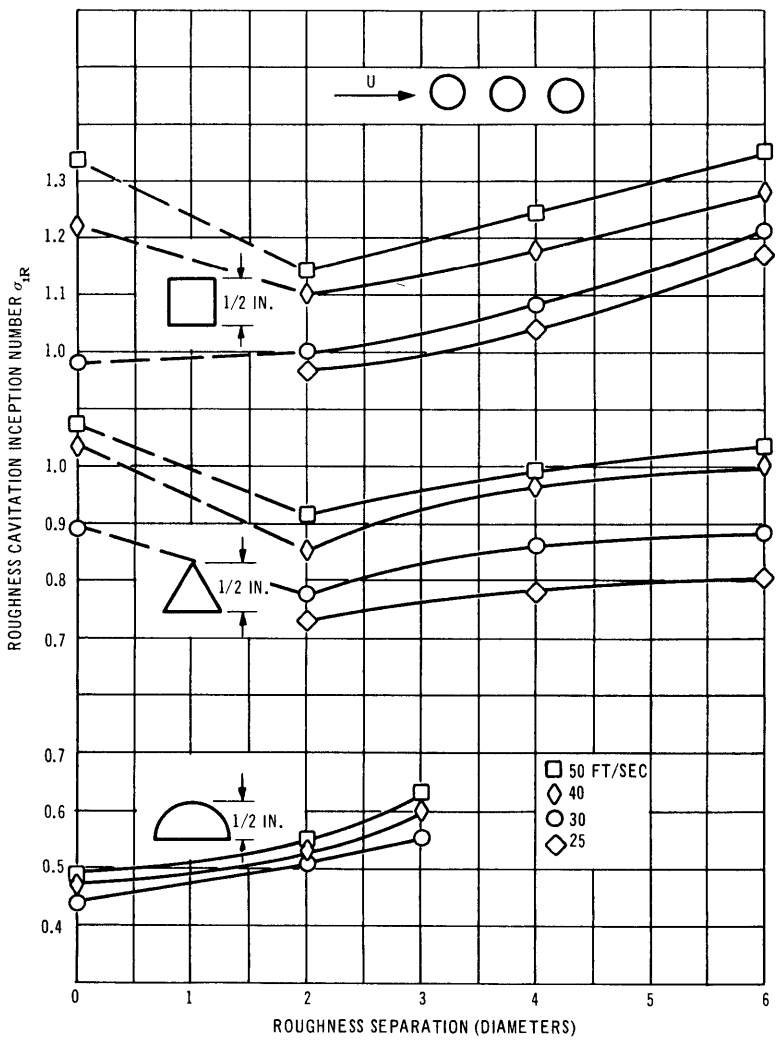

Figure 15 - Cavitation Inception Number as a Function of Longitudinal Roughness Separation

DISCUSSION

Cavitation can be generally defined as the growth of microscopic, undissolved air nuclei into vapor or gas filled voids in a liquid when the static pressure is dynamically reduced to or below a critical value, e.g., the vapor pressure of the liquid. Cavitation will appear on a moving body when its speed is sufficient to reduce the hydrodynamic pressure, over a portion of the body, to the critical value. As nuclei pass into this low pressure region, they grow and explode as a result of air diffusion and liquid evaporation. Downstream of the critical pressure region, the cavity collapses and air nuclei trail off into the wake. If the surface of the body is rough, the individual roughness protrusions will cause a further reduction in the hydrodynamic pressure which will result in cavitation inception at a lower speed than that of the smooth body. As the ratio of the roughness height to boundary layer thickness increases, the roughness element extends into a higher velocity region of the boundary layer and creates a greater reduction in the wake pressure. The shape of the boundary layer velocity profile is also an important parameter since the "fuller" profiles are characterized by a larger mean velocity component at any particular distance above the flow surface. The sensitivity of cavitation inception to the geometry of the roughness is evident in a comparison of Figures 11, 12, and 13.

BOUNDARY LAYER DETERMINATION

In phase I, the boundary layer thickness, δ, at the test station on the plate, was observed to grow with an increase in velocity. That is, δ increased from about 1.12 inches to 1.22 inches as the velocity was increased from 20 ft/sec to 60 ft/sec (see Figure 8). The growth of the boundary layer was a result of a forward shift of the turbulence transition point with the increase in tunnel velocity. This forward shift was probably accelerated by an increase in free-stream turbulence intensity resulting from the chopping action of the water circulating impeller. This trend is opposite from that predicted from the Blasius turbulent boundary layer approximation:

$$\delta(x) = 0.37 \times \left(\frac{Ux}{\nu}\right)^{-\frac{1}{5}} \qquad [7]$$

where x is the position downstream from the leading edge. Some idea of the magnitude of the effect of the shifting transition point is seen in Table 2, in which a comparison is made between measured and calculated values of the boundary layer thickness.

The power of Equation [3] was determined from the average of the slopes, m, of the straight line plots in Figure 7. Values of m obtained for various free-stream velocities are listed in Table 3. The solid line in Figure 9 is a plot of the power law:

$$\frac{u}{U} = \left(\frac{y}{\delta}\right)^{1/6.67} \qquad [8]$$

The working section of the water tunnel has a slight divergence in the down-stream direction, the purpose of which is to regain static pressure lost to friction as the water passes through the section. The manufacturer's calibration[2] of the prototype (or model) shows very little pressure loss through this tunnel section. The presence of the flat plate in the tunnel doesn't seem to alter the situation because the observed longitudinal pressure gradient was negligible.

CAVITATION INCEPTION

Cavitation begins with the growth of small air bubbles or nuclei. These nuclei are stabilized in organic films[3] which ultimately thicken and tend to seal off further diffusion of gas or the gas is entrapped in unwetted crevices in solid surfaces and even in suspended solids in the liquid. The presence of these nuclei is necessary for rupture of the liquid to occur at pressures of the order of the local vapor pressure. Experiments have shown that air-saturated, but denucleated, water exhibits high tensile strengths. In natural water, however, the tensile properties are negligible.

Although this report is concerned with cavitation inception, it should be noted here that the data points are actually points of cavitation

TABLE 2

Measured versus Calculated Boundary Layer Thickness

δ / U	Measured	Calculated
20 ft/sec	1.14 in.	1.29 in.
60 ft/sec	1.21 in.	1.034 in.

TABLE 3

Determination of the Power, m

Free-Stream Velocity, U	20	25	30	35	40	45	50	55	60
Power, m	6.7	6.58	6.95	6.16	6.54	6.39	6.80	6.85	7.05
Average m = 6.67									

disappearance or "desinence" as defined by Holl.[1] The difference, if any, between incipient and desinent cavitation is referred to as hysteresis. Observance of a lag or hysteresis between cavity appearance and disappearance seems to depend on the experimental technique used.

In a recent paper, Holl[4] develops several relations between hysteresis and total air content, surface materials, etc. His technique for achieving cavitation inception on a body was to hold the velocity fixed and rapidly drop the static pressure of the water tunnel from a predetermined value above the cavitation pressure to a series of values below the cavitation pressure. He then measured the time interval until cavitation appeared. Using the above technique, Holl observed that the time interval to inception varied with the tunnel velocity, air content, size of cavitating model, surface characteristics of the model, etc. Holl's general conclusion is that cavitation hysteresis is strictly random. The implication in these observations is that cavitation inception occurs upon the statistical arrival of an air nucleus whose size and tensile characteristics are such that it will "explode" on passing through the particular low pressure region being generated. Both Holl[4] and Straub[5] theorize that hysteresis is a function of the pressure history or preconditioning of the nuclei. Under experimental conditions where hysteresis has been observed, the incipient cavitation number σ_{iR}, is less than the desinent cavitation number σ_{dR}. To achieve cavitation inception in a water tunnel, the common procedure is to fix the velocity and to lower the static pressure slowly until the cavity appears. The relatively small air nuclei, passing through the test section, are simultaneously growing and diffusing gas to adjust to the decreasing ambient pressure. To cause an established cavity to disappear, the reverse procedure is followed and the nuclei may be decreasing from a relatively large size. The hysteresis phenomena coincides with Knapp's[6] observation that the effective tensile strength of the water is increased by pressurization. That is, a small bubble associated with a high pressure history exhibits higher surface tension forces and smaller air diffusion rates than a larger bubble associated with the lower pressure.

Since the occurrence of hysteresis seems to depend on pressure exposure and rapid pressure changes, the elimination of hysteresis may be accomplished by limiting the rate of pressure change in the flowing system. In the present experiment, the pressure change was slow enough that little difference was observed between the points of inception and disappearance of cavitation on a roughness. However, the point of disappearance of the cavity was used for convenience. A cavity could be readily established, reduced to a minimum size, and held fixed for a predetermined period while the tunnel nuclei stabilized to the new ambient conditions. The pressure was then increased, but through a very small pressure change, until the cavity disappeared. Ripken[7] has observed that about three minutes are required for free gas bubbles or nuclei to achieve stability after a change in tunnel pressure, "either large or small." When the above procedure was followed, the cavitation inception number, σ_{iR}, and cavitation desinence number, σ_{dR}, were effectively equal. One indication of the equality of these two numbers was the flickering in and out of the cavity with the slow oscillations in the tunnel static pressure.

In the course of this investigation several interesting effects were observed. For any particular roughness geometry the roughness cavitation inception number increased with the relative roughness height, h/δ. As the element extends further into the high velocity flow of the boundary layer, the critical mean velocity for cavitation inception is produced by a lower free-stream velocity. This is clearly shown in Figures 11, 12, and 13. Furthermore, a sharp-edged roughness, where the cavity forms in the separation region, cavitates at lower velocities than a smooth roughness of the same height. In this experiment the highest cavitation numbers (the worst case) was generated by the right circular cylinder which presented a vertical profile and sharp rim to the flow.

Each of the roughness elements investigated have sharp pressure minima at their tips. The sketches in Figure 16 illustrate how the last traces of cavitation were found in those areas of high shear where the flow tends to separate into a vortex sheet. The photographs in Figure 17 show several shapes and sizes of roughness elements under exaggerated cavitation conditions. One very interesting phenomenon was the appearance of a horseshoe vortex which occurred with the spherical roughness. Such

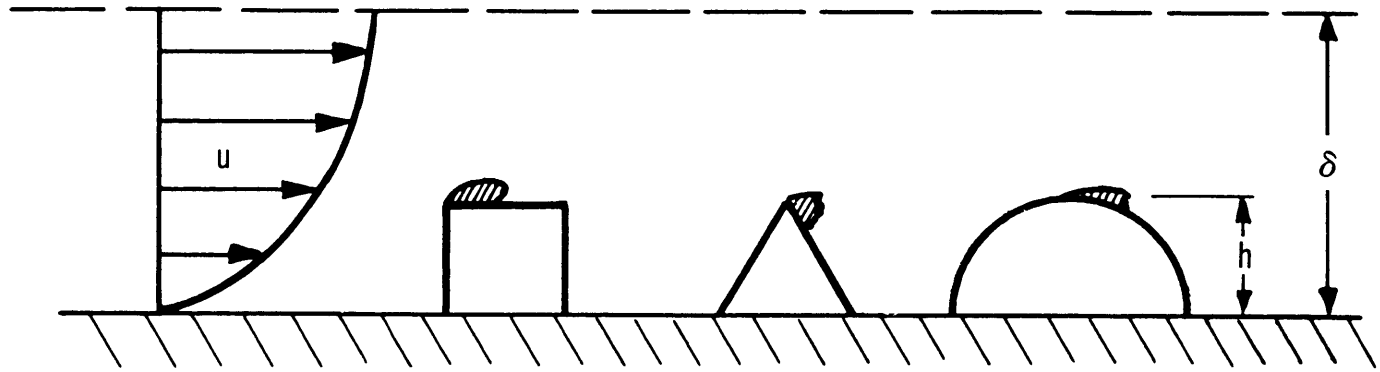

Figure 16 - Last Traces of Cavitation
on Roughnesses

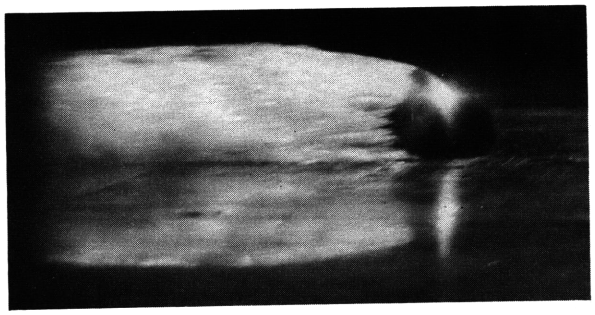

Figure 17a

Figure 17b

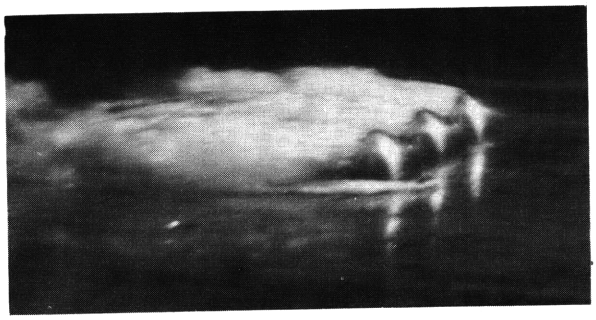

Figure 17c

Figure 17d

Figure 17e

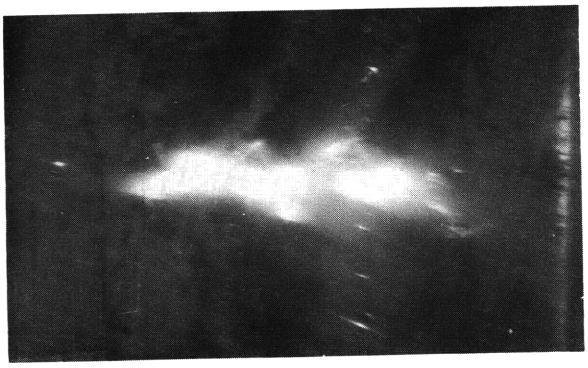

Figure 17f

Figure 17 - Fully Cavitating Flow (Note "Horse-shoe" Vortex on Hemispherical Roughnesses)

vortices were also observed by Thwaites[10] about cylindrical bumps in a laminar boundary layer. Although vortex flow exists around the base of all the elements, the pressure configurations were such that only in the case of the larger hemispheres did the vortex core cavitate and become visible.

When a roughness element protrudes into a boundary layer, the flow is accelerated over the top and around the sides of the element, but is retarded in the near wake. Because of the low pressure in the wake, high velocity streamlines are deflected downward aft of the roughness and produce an increased flow velocity which extends some distance downstream. In the transverse pattern, acceleration of fluid around the sides of one element influences the fluid velocity in the vicinity of neighboring elements. As seen in Figure 14, when there were three roughnesses in a line normal to the flow, the cavitation number for inception on one of the elements in the group increased as the spacing between the elements decreased. However, after the initial cavity appeared on any one of the elements, the local pressure increased and a higher flow velocity was required before the neighboring elements cavitated. When the three elements were alligned with the flow, initial signs of cavitation consistently appeared on the last element in the row [downstream]. In the spread out longitudinal configuration, setting 1 of Figure 5, the downstream element was subjected to the low pressure, high velocity wake generated by the forward element. However, decreasing the spacing between elements lowered the incipient cavitation number because the downstream elements were moved into the lower velocity region of the near wake of the forward elements. Consequently, the external flow velocity had to be increased to achieve cavitation as the roughness spacing was decreased. Again, the presence of a cavity on the rear element caused an increase in the local pressure and a divergence of the flow lines forward of the element so that an increase in the external flow velocity was required to cause the remaining elements to cavitate. In References 8 and 9, Schlichting discusses experimental observations of wake velocities of roughnesses in a boundary layer.

In both the normal and longitudinal patterns, there was a sizeable difference between the velocity at which initial cavitation appeared (on

one element) and that at which the remaining elements began to cavitate. In Figures 14 and 15, the incipient cavitation number for these patterns refers to the point at which cavitation initially appeared on one of the elements. The point at which all three elements achieved cavitation was erratic and ill-defined. Figure 17 shows fully developed cavitation over several patterns of roughness elements.

Figure 14 shows the change in inception cavitation number for the normal pattern. The cavitation numbers have maximum values at the smallest spacings but approach the single-element values at 6 diameters. Figure 15 shows the change in inception cavitation number when the elements are aligned with the flow. The cavitation number is generally reduced when the elements are close together but increase to the single-element value as the spacing increases.

The cavitation inception numbers of single roughness elements were observed for varying air contents of 12 to 54 percent of saturation of the tunnel water. For this increase in air content, an increase in σ_{iR} of about 7 percent was noticed in the case of the one-half inch circular cylinder. However, these data were scattered and inconclusive. Holl[1] similarly experienced a slight increase in σ_{iR} with air content in the case of the triangular, two-dimensional roughness.

SCALING

The ultimate purpose of this experiment is to develop data for predicting cavitation inception resulting from roughness elements on full-scale flow surfaces. Inasmuch as the data from this investigation apply to roughness elements in only one particular boundary layer, it is important to present the data in terms of local flow conditions at the point of cavitation inception. For this purpose local Reynolds numbers and local cavitation numbers were computed by the following formulas:

Local Reynolds number $$R_h = h\, u_h/\nu \qquad [9]$$

Local cavitation number $$\sigma_h = \frac{p - p_v}{1/2\, \rho\, u_h^2} \qquad [10]$$

where u_h is the flow velocity at the height of the roughness

ν is the kinematic viscosity of the liquid

If the data in Figures 11 through 13 are plotted as functions of σ_h and R_h on log-log paper, a straight line can be drawn through the points for each roughness geometry. These plots are shown in Figure 18. Since all the tests were run at essentially the same temperature, 78 degrees F, the present work does not prove that this is a true Reynolds number effect. In fact, data for each roughness size show systematic deviations from the average trend. Such factors as heat transfer, nuclear content, etc. follow different scaling laws.[12] On the other hand, a much larger cylinder was recently tested for cavitation inception in the TMB towing basin. This cylinder was 8 inches in diameter and 6 inches high. Cavitation occurred at 16 knots at the tip which was 4.5 ft below the surface. The cavitation point for this cylinder falls almost on the straight line fitted to the small cylinder data; see Figure 18.

In Reference 13 Holl's two-dimensional data have been reduced in terms of the local cavitation number and local Reynolds number. Although these data were obtained in four different boundary layers and in two different water tunnels, the reduced data for each of his roughness geometries gave a similar relationship. The effects of roughness height and boundary layer profile were of minor importance compared with the Reynolds number dependence.

Reynolds number scaling has also definitely been found in tests on ogive and other bluff bodies in which the temperature was varied from 52 to 99 degrees F.[12] On the other hand, no definite Reynolds number effect was found on certain airfoil sections or on bodies which had broad pressure minima. In these cases the point of cavitation inception fluctuated and cavitation inception appeared to be more dependent on the characteristics of the entrained air in the flow.

In the TMB experiments cavitation inception always occurred in a sharp low pressure region where the flow would naturally separate. McCormick[12] has suggested that the cavity forms in the core of a vortex sheet where the pressure reduction is a function of the product of the velocity and a representative length. He further postulated that the thickness of the vortex sheet boundary layer is a viscous phenomenon and that a Reynolds number effect may be expected.

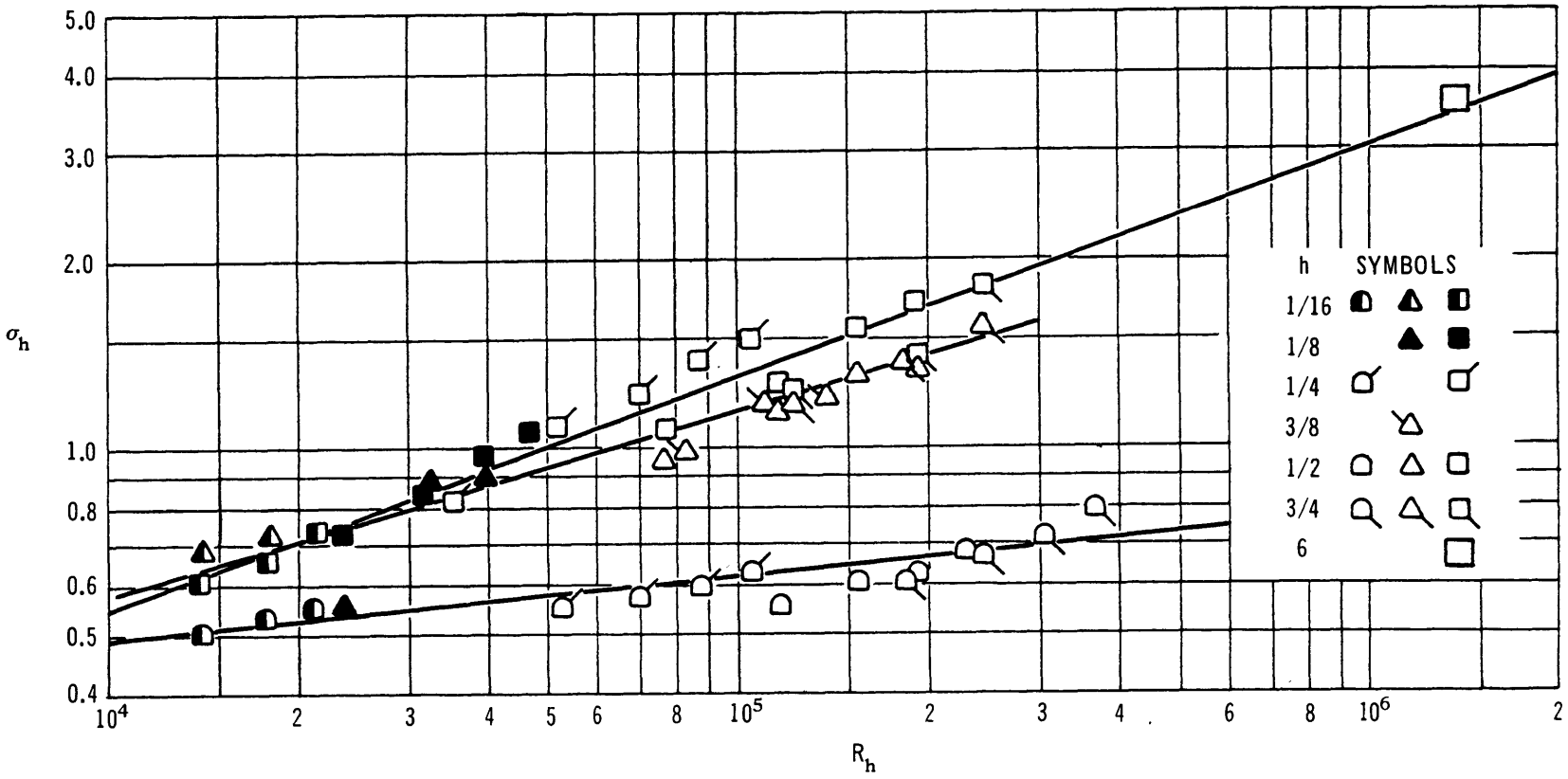

Figure 18 - Local Cavitation Number as Function of Local Reynolds Number

CONCLUSIONS

The boundary layer characteristics of the flow, 8 ft from the leading edge of a flat plate in the TMB 36-Inch Water Tunnel, may be summarized as follows:

1. The boundary layer thickness, δ, increased from 1.12 to 1.22 inches as the velocity was increased from 20 to 60 ft/sec; see Figure 8.

2. The measured velocity profile closely approximated a power law representation with exponent 6.67.

3. The longitudinal pressure gradient along the surface of the plate was negligible.

Cavitation properties of three geometries of roughness elements embedded in a boundary layer may be summarized as follows:

1. For each roughness geometry, the cavitation inception number, σ_{iR}, increases with the relative roughness height h/δ.

2. For each roughness geometry, σ_{iR} increases with the tunnel velocity U.

3. Among the various roughness geometries σ_{iR} increases with the "sharpness" of the element. Under similar conditions σ_{iR} was always largest for the circular cylinder and smallest for the hemisphere.

4. A cavitation horseshoe vortex was observed at the base of the larger hemispherical roughness elements. None was observed with the cone or cylinder.

5. In transverse roughness patterns, σ_{iR} increased with a decrease in element separation.

6. In longitudinal roughness patterns, σ_{iR} increased with an increase in element separation.

7. A 40 percent increase in air content did not conclusively alter the cavitation inception characteristics of the roughnesses.

8. For each of the bluff roughness elements tested, local cavitation number, σ_h, showed a systematic variation with local Reynolds number, R_h.

REFERENCES

1. Holl, J.W., "Inception of Cavitation on Isolated Surface Irregularities," ASME Journal of Basic Engr., Mar 1960.

2. Brownell, W.F., "A 36-Inch Variable Pressure Water Tunnel," TMB Report 1052, Jun 1956.

3. Fox, Francis E., and Herzfeld, Karl F., "Gas Bubbles with Organic Skin as Cavitation Nuclei," Journal of Acoustical Society of America, Vol 26, No. 6, 984 - 989, Nov 1954.

4. Holl, J.W., and Treaster, A.L., "Cavitation Hysteresis," ASME Paper No. 65 FE-9.

5. Straub, L.G., "A Study of the Influence of Gas Nuclei on Cavitation Scale Effects in Water Tunnel Tests," St. Anthony Falls Hydraulic Laboratory, Project Report No. 58, Feb 1958.

6. Knapp, R.T., "Cavitation and Nuclei," Trans. ASME, Vol. 80, 1958, pp. 1315 - 1324.

7. Ripken, J.F. and Killen, J.M., "Gas Bubbles: Their Occurrence, Measurement, and Influence in Cavitation Testing," IAHR Symposium on Cavitation and Hydraulic Machinery, Paper No. A-3, Sept 1962.

8. Schlichting, H., "Boundary Layer Theory," McGraw Hill, 4th Edition, 1960.

9. Schlichting, H., "Experimental Investigation of the Problem of Surface Roughness," NACA TM No. 823.

10. Thwaites, B., "Incompressible Aerodynamics," Oxford, 1960 (Clarendon Press).

11. Streeter, Victor L., "Handbook of Fluid Dynamics, First Edition McGraw Hill, 1961.

12. Holl, J.W. and Wislicenus, G.F., "Scale Effects on Cavitation," Transactions of the ASME Journal of Basic Engineering, p 385, Sept 1961.

13. Borden, A., "Prediction of Cavitation Inception Speeds on Rough Bodies," David Taylor Model Basin Report (in preparation)

INITIAL DISTRIBUTION

Copies	
12	CHBUSHIPS 3 Tech Lib (Code 210L) 1 Hydro, Logistics & Spec. Craft Sec (Code 341B) 1 Materials, Fuels & Cold Weather Sec (Code 342A) 1 Ship Sil Br (Code 345) 1 Hull Des Br (Code 440) 1 Scien & Res Sec (Code 442) 1 Cruisers & Dest Br (Code 523) 1 Materials & Chem Br (Code 634) 2 AN/SQS-26 Sonar Sys Proj Office (Code 1631)
20	DDC
1	CHBUWEPS
1	CHONR Mech Br (Code 438)
1	DIR USNRL
1	CDR USNOL, White Oak
1	CDR USNOTS, China Lake
1	USNUSL
1	USNMEL
1	NAVSHIPYD BSN
1	NAVSHIPYD CHASN
1	NAVSHIPYD LBEACH
1	NAVSHIPYD MARE
1	NAVSHIPYD NYK
1	NAVSHIPYD NORVA
1	NAVSHIPYD PEARL
1	NAVSHIPYD PHILA
1	NAVSHIPYD PTSMH
1	NAVSHIPYD PUG
1	NAVSHIPYD SFRAN
1	SUPSHIP, Bath
1	SUPSHIP, Bay City
1	SUPSHIP, Camden
1	SUPSHIP, Groton

Copies	
1	SUPSHIP, Long Beach
1	SUPSHIP, Newport News
1	SUPSHIP, New York
1	SUPSHIP, Pascagoula
1	SUPSHIP, San Francisco
1	SUPSHIP, Seattle
1	SUPSHIP, New Orleans
1	Supt, USNA Attn: Library
1	Supt, NAVPGSCOL
1	CMDT, USCG
1	CDR, MSTS
2	Admin, MARAD Attn: Div of Ship Design Div of Research
1	CO & DIR, USNMDL
1	CO, USNROTC & NAVADMINU, MIT
1	Dir Eng Sciences Div National Science Foundation
1	Dir, Natl BuStand Attn: Fluid Mechanics Div (Dr. G.B. Schubauer)
1	OTS, Dept Comm
2	State Univ of Iowa Iowa Institute of Hydraulic Research Attn: Dr. H. Rouse Dr. L. Landweber
1	HD, Dept NAME, Univ of Michigan, Ann Arbor
1	Dir, St. Anthony Falls Hydraulic Lab, Univ of Minn
1	Prof J.J. Foody, Eng Dept, New York State Univ Maritime College Fort Schulyer, N.Y.

Copies	
3	Dir, ORL, Penn State Attn: Dr. M. Sevik Dr. J.W. Holl Dr. G.F. Wislicenus
1	Dir, Davidson Lab, SIT, Hoboken Attn: Dr. J.P. Breslin
3	O in C, PGSCOL, Webb Attn: Prof E.V. Lewis Tech Lib
1	EB Div/GD Corp
1	Gibbs & Cox, Inc.
2	Dir, SWRI Attn: Dr. H.N. Abramson
1	Hydronautics, Inc. Attn: Mr. Phillip Eisenberg
1	Oceanics, Inc. Technical Industrial Park Plainview, N.Y.
1	Colorado State Univ Fort Collins, Colorado Dept of Civil Engin
1	CIT, Pasadena Attn: Prof. M.S. Plesset
3	MIT, Dept NAME Prof. A.T. Ippen Prof. M.A. Abkowitz
1	NNSB & DDCo C.H. Hancock Hydraulic Lab & Ship Model Testing Tank
2	Dr. E.Y. Hsu Dept of Civil Eng Stanford Univ Stanford, California
1	Prof L.J. Hooper Alden Hydraulic Lab Worcester Polytechnic Inst Worcester 2, Mass
1	O in C USNOTS, Pasadena
1	CO, USNUOS Mr. R.J. Grady
1	TRG, Inc.

Copies	
1	Dir, WHOI
1	Scripps Inst of Oceanography Univ of Calif LaJolla, Calif
1	Lockheed Aircraft Corp Missiles & Space Div Palo Alto, Calif
1	Head, Dept of Mech Eng Purdue Univ Lafayette, Indiana

Unclassified
Security Classification

DOCUMENT CONTROL DATA - R&D

(Security classification of title, body of abstract and indexing annotation must be entered when the overall report is classified)

1. ORIGINATING ACTIVITY *(Corporate author)* David Taylor Model Basin Washington, D.C. 20007	2a. REPORT SECURITY CLASSIFICATION Unclassified 2b GROUP

3 REPORT TITLE

CAVITATION INCEPTION ON THREE-DIMENSIONAL ROUGHNESS ELEMENTS

4 DESCRIPTIVE NOTES *(Type of report and inclusive dates)*

Final

5 AUTHOR(S) *(Last name, first name, initial)*

Benson, Bruce W.

6. REPORT DATE	7a TOTAL NO. OF PAGES	7b. NO OF REFS
May 1966	35	13

8a. CONTRACT OR GRANT NO. b. PROJECT NO. S-F013 02 04 Task 1712 c. d.	9a. ORIGINATOR'S REPORT NUMBER(S) 2104 9b. OTHER REPORT NO(S) *(Any other numbers that may be assigned this report)*

10. AVAILABILITY/LIMITATION NOTICES

Distribution of this document is unlimited.

11 SUPPLEMENTARY NOTES	12. SPONSORING MILITARY ACTIVITY
	Naval Ship Systems Command, Code 6420 Washington, D.C.

13 ABSTRACT

Cavitation inception velocities have been measured for the flow over three-dimensional roughness elements, embedded in a boundary layer on a flat plate, in the 36-inch water tunnel at the David Taylor Model Basin. The roughness elements considered are right circular cylinders, cones, and hemispheres whose heights vary from one-thirty-second to three-forths of an inch. Cavitation inception number, based on tunnel velocity, is plotted as a function of the ratio of roughness height to boundary layer thickness. This resulted in separate curves for each test velocity. When, however, the cavitation number was computed on the basis of the velocity within the boundary layer at the tip of the roughness, the cavitation number was found to be primarily a function of the local Reynolds number, based on roughness height and local velocity. Of the three roughness geometries, the cylinders produced the largest cavitation numbers; the hemispheres, the smallest.

DD FORM 1 JAN 64 1473

Unclassified
Security Classification

14. KEY WORDS	LINK A		LINK B		LINK C	
	ROLE	WT	ROLE	WT	ROLE	WT
Cavitation inception Incipient cavitation number Rough surface Roughness height Relative height Boundary layer thickness Flat plate Velocity profile Hydrodynamic shape Air nuclei Air content Water tunnel Manometer Pitot tube						

INSTRUCTIONS

1. ORIGINATING ACTIVITY: Enter the name and address of the contractor, subcontractor, grantee, Department of Defense activity or other organization *(corporate author)* issuing the report.

2*a*. REPORT SECURITY CLASSIFICATION: Enter the overall security classification of the report. Indicate whether "Restricted Data" is included. Marking is to be in accordance with appropriate security regulations.

2*b*. GROUP: Automatic downgrading is specified in DoD Directive 5200.10 and Armed Forces Industrial Manual. Enter the group number. Also, when applicable, show that optional markings have been used for Group 3 and Group 4 as authorized.

3. REPORT TITLE: Enter the complete report title in all capital letters. Titles in all cases should be unclassified. If a meaningful title cannot be selected without classification, show title classification in all capitals in parenthesis immediately following the title.

4. DESCRIPTIVE NOTES: If appropriate, enter the type of report, e.g., interim, progress, summary, annual, or final. Give the inclusive dates when a specific reporting period is covered.

5. AUTHOR(S): Enter the name(s) of author(s) as shown on or in the report. Enter last name, first name, middle initial. If military, show rank and branch of service. The name of the principal author is an absolute minimum requirement.

6. REPORT DATE: Enter the date of the report as day, month, year; or month, year. If more than one date appears on the report, use date of publication.

7*a*. TOTAL NUMBER OF PAGES: The total page count should follow normal pagination procedures, i.e., enter the number of pages containing information.

7*b*. NUMBER OF REFERENCES: Enter the total number of references cited in the report.

8*a*. CONTRACT OR GRANT NUMBER: If appropriate, enter the applicable number of the contract or grant under which the report was written.

8*b*, 8*c*, & 8*d*. PROJECT NUMBER: Enter the appropriate military department identification, such as project number, subproject number, system numbers, task number, etc.

9*a*. ORIGINATOR'S REPORT NUMBER(S): Enter the official report number by which the document will be identified and controlled by the originating activity. This number must be unique to this report.

9*b*. OTHER REPORT NUMBER(S): If the report has been assigned any other report numbers *(either by the originator or by the sponsor)*, also enter this number(s).

10. AVAILABILITY/LIMITATION NOTICES: Enter any limitations on further dissemination of the report, other than those imposed by security classification, using standard statements such as:

(1) "Qualified requesters may obtain copies of this report from DDC."

(2) "Foreign announcement and dissemination of this report by DDC is not authorized."

(3) "U. S. Government agencies may obtain copies of this report directly from DDC. Other qualified DDC users shall request through _____."

(4) "U. S. military agencies may obtain copies of this report directly from DDC. Other qualified users shall request through _____."

(5) "All distribution of this report is controlled. Qualified DDC users shall request through _____."

If the report has been furnished to the Office of Technical Services, Department of Commerce, for sale to the public, indicate this fact and enter the price, if known.

11. SUPPLEMENTARY NOTES: Use for additional explanatory notes.

12. SPONSORING MILITARY ACTIVITY: Enter the name of the departmental project office or laboratory sponsoring *(paying for)* the research and development. Include address.

13. ABSTRACT: Enter an abstract giving a brief and factual summary of the document indicative of the report, even though it may also appear elsewhere in the body of the technical report. If additional space is required, a continuation sheet shall be attached.

It is highly desirable that the abstract of classified reports be unclassified. Each paragraph of the abstract shall end with an indication of the military security classification of the information in the paragraph, represented as *(TS)*, *(S)*, *(C)*, or *(U)*.

There is no limitation on the length of the abstract. However, the suggested length is from 150 to 225 words.

14. KEY WORDS: Key words are technically meaningful terms or short phrases that characterize a report and may be used as index entries for cataloging the report. Key words must be selected so that no security classification is required. Identifiers, such as equipment model designation, trade name, military project code name, geographic location, may be used as key words but will be followed by an indication of technical context. The assignment of links, roles, and weights is optional.

David Taylor Model Basin. Report 2104.
CAVITATION INCEPTION ON THREE-DIMENSIONAL ROUGHNESS ELEMENTS, by Bruce W. Benson. May 1966. iii, 32p. illus., diags., graphs. refs. UNCLASSIFIED

Cavitation inception velocities have been measured for the flow over three-dimensional roughness elements, embedded in a boundary layer on a flat plate, in the 36-inch water tunnel at the David Taylor Model Basin. The roughness elements considered are right circular cylinders, cones, and hemispheres whose heights vary from one-thirty-second to three-forths of an inch. Cavitation inception number, based on tunnel velocity, is plotted as a function of the ratio of roughness height to boundary layer thickness. This resulted in separate curves for each test velocity. When, however, the

1. Cavitation--Inception--Prediction
2. Plates--Roughness elements--Cavitation
I. Benson, Bruce W.
II. S-F013 02 04; Task 1712

David Taylor Model Basin. Report 2104.
CAVITATION INCEPTION ON THREE-DIMENSIONAL ROUGHNESS ELEMENTS, by Bruce W. Benson. May 1966. iii, 32p. illus., diags., graphs. refs. UNCLASSIFIED

Cavitation inception velocities have been measured for the flow over three-dimensional roughness elements, embedded in a boundary layer on a flat plate, in the 36-inch water tunnel at the David Taylor Model Basin. The roughness elements considered are right circular cylinders, cones, and hemispheres whose heights vary from one-thirty-second to three-forths of an inch. Cavitation inception number, based on tunnel velocity, is plotted as a function of the ratio of roughness height to boundary layer thickness. This resulted in separate curves for each test velocity. When, however, the

1. Cavitation--Inception--Prediction
2. Plates--Roughness elements--Cavitation
I. Benson, Bruce W.
II. S-F013 02 04; Task 1712

David Taylor Model Basin. Report 2104.
CAVITATION INCEPTION ON THREE-DIMENSIONAL ROUGHNESS ELEMENTS, by Bruce W. Benson. May 1966. iii, 32p. illus., diags., graphs. refs. UNCLASSIFIED

Cavitation inception velocities have been measured for the flow over three-dimensional roughness elements, embedded in a boundary layer on a flat plate, in the 36-inch water tunnel at the David Taylor Model Basin. The roughness elements considered are right circular cylinders, cones, and hemispheres whose heights vary from one-thirty-second to three-forths of an inch. Cavitation inception number, based on tunnel velocity, is plotted as a function of the ratio of roughness height to boundary layer thickness. This resulted in separate curves for each test velocity. When, however, the

1. Cavitation--Inception--Prediction
2. Plates--Roughness elements--Cavitation
I. Benson, Bruce W.
II. S-F013 02 04; Task 1712

cavitation number was computed on the basis of the velocity within the boundary layer at the tip of the roughness, the cavitation number was found to be primarily a function of the local Reynolds number, based on roughness height and local velocity. Of the three roughness geometries, the cylinders produced the largest cavitation numbers; the hemispheres, the smallest.

cavitation number was computed on the basis of the velocity within the boundary layer at the tip of the roughness, the cavitation number was found to be primarily a function of the local Reynolds number, based on roughness height and local velocity. Of the three roughness geometries, the cylinders produced the largest cavitation numbers; the hemispheres, the smallest.

cavitation number was computed on the basis of the velocity within the boundary layer at the tip of the roughness, the cavitation number was found to be primarily a function of the local Reynolds number, based on roughness height and local velocity. Of the three roughness geometries, the cylinders produced the largest cavitation numbers; the hemispheres, the smallest.